Anthropogenic aerosol optical depth during days of high haze levels in the Beijing winter

WANG Yan[1], XIE Yisong[1,2], LI Zhengqiang[1], LI Donghui[1,2], LI Kaitao[1,2]

1. *State Environmental Protection Key Laboratory of Satellite Remote Sensing, Institute of Remote Sensing and Digital Earth, Chinese Academy of Sciences, Beijing* 100101, *China*;
2. *University of Chinese Academy of Sciences, Beijing* 100049, *China*

Abstract: we estimated anthropogenic contributions to Aerosol Optical Depth (AOD) during days of high haze level using ground-based measurements in Beijing (January 2009 and 2013). We compared the anthropogenic AOD (AOD_{an}) with optical p arameters determined directly from aerosol samples. The results showed: (1) The monthly mean AOD_{an} (at 440 nm) of January was 0.88 in 2009 and 0.44 in 2013; (2) The proportion of days where contributions from AOD_{an} dominated in January 2013 was 86.7%, higher than that in January 2009 (62.5%); (3) The ratio of the AOD_{an} to total AOD (at 440 nm) was about 88% in January 2013, indicating the importance of the anthropogenic aerosol contribution to haze pollution; (4) The two haze events studied featured c ontributions from accumulation of local pollutants and pollutants transported from surrounding areas of Beijing.

Key words: anthropogenic aerosol optical depth, haze, aerosol accumulation mode fraction, aerosol from ground-based observation

CLC number: TP701 **Document code:** A

Citation format: **Wang Y, Xie Y S, Li Z Q, Li D H and Li K T. 2013. Anthropogenic aerosol optical depth during days of high haze levels in the Beijing winter. Journal of Remote Sensing, 17(4): 993-1007 [DOI: 10.11834/jrs.20133071]**

1 INTRODUCTION

Haze pollution is a significant hazard to public health, and is a topic of growing public concern. Owing to rapid growth of population and the number of motor vehicles over the last 20 years, Beijing, as the largest city in North China, has suffered the effects of serious anthropogenic pollution. Following the 2008 Beijing Olympic Games, the air quality of Beijing has declined with frequent and severe haze pollution incidents in autumn and winter, particularly in February 2011 and 2012 (Li, et al., 2013). Statistics show that during January 2013, the conditions of only five days satisfied environmental standards. Many scientists had studied the optical properties of aerosol haze pollution and several researchers have studied the anthropogenic AOD during days of intense haze (Yan, 2010; Yu, 2012; Wang, 2009).

The aerosols can be divided into two different sources, n atural and man-made aerosols. Natural aerosols consist primarily of large dust particles and sea salt. Anthropogenic aerosols are emissions from human activities consisting of small sized particulate matter, including sulfates, nitrates, carbon black and organic carbon. There has been a large amount of research concerning anthropogenic aerosols, radiative forcing and climatic effects (Sun, et al., 2008a, 2008b).

Researchers may use remote sensing techniques to distinguish between natural and anthropogenic aerosols using the Accumulation Mode Fraction (AMF). AMF is defined as the proportion of fine modal aerosol optical thickness of the total optical thickness (O'Neill, 2003). Generally, AMFs > 0.83 are classified as anthropogenic aerosols, and the AMFs < 0.35 are classified as natural aerosols (Bellouin, et al., 2005).

In this paper, the AMF method is extended for use with ground-based remote sensing data to estimate the anthropogenic aerosol optical thickness during haze pollution events in Beijing in January 2013. We also compare these finding with calculations based upon results from January 2009.

2 DATA AND METHODS

2.1 Observation data

In this study, we used the AERONET (AErosol RObotic NETwork) data of Beijing site (39.98°N, 116.38°E, Altitude: 95 m) in January 2009 and January 2013. AERONET is a global aerosol monitoring network, initiated by NASA (Holben et al., 2001) and PHOTONS (Goloub, et al., 2008) and has greatly e xpanded over the years through the participation of collaborators around the world. AERONET aerosol data are widely used by the atmospheric science community to characterize aerosol properties (Schuster, et al., 2009; Dubovik, et

Received: 2013-03-26; **Accepted:** 2013-05-14; **Version of record first published:** 2013-05-21

Foundation: National Major Scientific Research Program (No. 2010CB950800, 2010CB950801); Strategic Priority Research Program of the Chinese Academy of Sciences (No. XDA05100202)

First author biography: WANG Yan (1974—), female, Ph. D., she majors in aerosol and the aerosol of radiative forcing. E-mail: wylf369@sina.com

Corresponding author biography: LI Zhengqiang (1977—), male, professor, his research interest is environment remote sensing. E-mail: lizq@irsa.ac.cn

al., 2000, 2006). The data used in this article include AOD, AMF, Single Scattering Albedo (SSA) and particle size distribution.

According to the Aid Quality Index (AQI) (API before 2013), clean weather conditions are defined by an AQI ≤100 and higher values denote polluted conditions. Air quality may be rated by other haze monitoring indicators such as humidity, visibility and particle size (Wu, 2007; China Meteorological Administration, 2010). By combining these standards with meteorological data, we select haze pollution events for study. Table 1 shows two different periods of weather pollution in January 2009 and 2013. In January 2009, unpolluted days in Beijing totaled 24 days, accounting for 77.4% of the month, with 0 day of moderate pollution. In January 2013, 10 unpolluted days accounted for only 32.2% of the month. Moderate pollution occurred on 16 days, accounting for 51.6% of the month. It is considered reasonable to select these two months to compare aerosol optical properties and anthropogenic aerosols.

Table 1 Weather pollution statistics in January 2009 and 2013 /d

	Excellent	Good	Slightly polluted	> Slightly polluted
2009	5	19	7	0
2013	3	7	6	15

2.2 Research Methods

In this paper, we used the Kaufman's algorithm (Kaufman, et al., 2005a, 2005b) and extended it to ground-based remote sensing observations, from which the anthropogenic aerosol properties were obtained in Beijing. We use the following assumptions to estimate the anthropogenic aerosol component:

(1) It is assumed that the aerosols may be divided into two kinds: anthropogenic and natural aerosols, where natural aerosols only include the dust and sea salt particulates while the anthropogenic aerosols are those generated by burning including smoke and pollution.

(2) The fractional contribution to the aerosol optical depth that arises from an aerosol is constant for a particular aerosol type (anthropogenic, dust, maritime). We represent the total aerosol optical depth τ_{550} by the sum of anthropogenic (air pollution and smoke aerosol) $-\tau_{anth}$, dust $-\tau_{dust}$, and baseline marine $-\tau_{mar}$, components:

$$\tau(\lambda) = \tau_{an}(\lambda) + \tau_{du}(\lambda) + \tau_{ma}(\lambda) \quad (1)$$

$$\tau_f(\lambda) = \tau(\lambda) \cdot \mathrm{AMF} \quad (2)$$

The Fine Aerosol Optical Depth ($\mathrm{AOD_f}$), calculated by the observed data can be described as:

$$\tau_f(\lambda) = f_{an}\tau_{an}(\lambda) + f_{du}\tau_{du}(\lambda) + f_{ma}\tau_{ma}(\lambda) \quad (3)$$

In Beijing winters, a northwesterly wind prevails such that transport of sea salt aerosols from the east and southeastern coast is rare. Thus, it may be further assumed that contribution of sea salt to the aerosol optical depth is 0, such that $\tau_{ma}(\lambda)$ equals 0. This assumption has little effect on the estimation of anthropogenic aerosols.

Based on the above analysis, we have two equations (Eq. (1) and Eq. (3)) and four unknown parameters. The parameters f_{du} and f_{an} are the dust and anthropogenic fine fractions respectively. The other parameters include the dust and anthropogenic aerosol optical depths. Kaufman (2005b) calculated the typical regional anthropogenic and dust aerosol proportions as 0.92 ± 0.03 and 0.51 ± 0.03, respectively.

There are two ways to get AMF parameters. The first method is based on the spectral distribution of the aerosol volume calculated directly using the Mie scattering theory to obtain AMF parameters ([2013-02-17] http://aeronet.gsfc.nasa.gov/cgi-bin/type_piece_of_map_opera_v2_inv2). The second approach is the use of 500 nm spectral deconvolution method for solving the AMF (O'Neill, et al., 2001, 2003; Zhang, et al., 2013). In this paper, we obtain the AMF of 440 nm values by the first method.

To verify whether the f_{an} and f_{du} values could be applied to this study, we selected a day of serious haze pollution (October 9, 2010) and a day of dust storms (April 17, 2004), and used the measured aerosol size distribution data to estimate the values of f_{an} and f_{du} from Mie scattering calculation.

We obtained the real particle spectral distribution by using an Aerodynamic Particle Size Spectrometer (APS3321) at Beijing University of Technology on October 9, 2010, and then calculated the f_{an} and f_{du}, as 0.92 and 0.50, respectively, in good agreement with the results of Kaufman (Kaufman, et al., 2005b). Therefore we use the values 0.92 and 0.50 for f_{an} and f_{du}, respectively, to estimate the anthropogenic aerosols in this work.

3 RESULTS AND ANALYSIS

3.1 The anthropogenic aerosol optical depth during haze pollution

Fig. 1 shows the total AOD, AMF and $\mathrm{AOD_{an}}$ at 440 nm over the month of January 2009 and January 2013. The daily mean AOD of January 2013 was 0.92, about 77% higher than the mean of January 2009, 0.52. Only two days with AOD greater than 1.0 occurred in January 2009, while four such days occurred in January 2013. The maximum AOD in 2013 reached 3.2, much higher than that of 1.7 in January 2009. The concentration of atmospheric aerosols in January 2013 was much higher than that of January 2009.

AMF parameters used to distinguish anthropogenic aerosols were significantly different over these two periods, as shown in Fig. 1(b). The minimum, maximum and monthly mean values of the AMF were 0.37, 0.93 and 0.83, respectively, in January 2009. In January 2013, the minimum, maximum and monthly mean values of the AMF were 0.62, 0.96 and 0.87, respectively, and significantly higher than those in 2009. During January 23 to 25, 2013, there was a significant decline in the process. The AMF in January 2013 remained above 0.8; only two days declined slightly to 0.6—0.7 (on January 8 and 24). According to the methods of Bellouin (Bellouin, 2005), there were 15 days of high anthropogenic aerosol levels (daily average AMF >0.83), accounting for 62.5% of the total days, 4.2% of which were days of high natural aerosol levels (daily average AMF value <0.35) in January 2009. Other days featured a mixture of natural and anthropogenic contributions, accounting for 33.3% of the total number of days. In January 2013, days of high an-

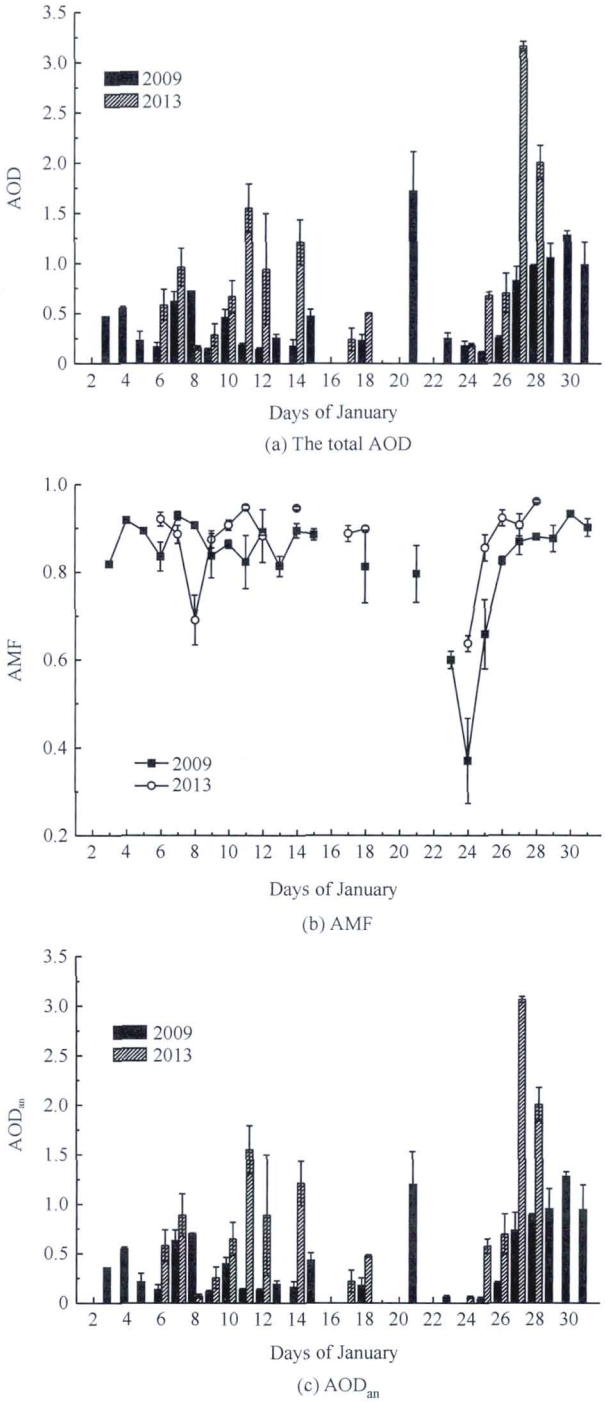

Fig. 1 The daily average AOD, AMF and AOD_{an} in January 2009 and 2003

thropogenic aerosol levels accounted for 86.7% of the total, mixed weather days accounted for 13.3% and there were no days with high natural aerosol levels.

Based on the method described in Section 2.2, we calculated the AOD_{an}. The AOD_{an} shows synchronous changes with AOD and AMF, which can be seen in Fig. 1(c). A decrease of AMF values corresponds with low AOD_{an} (January18 and 23 to 25, 2009 and January 8 and 24, 2013). From comparing AOD_{an} in January 2009 and 2013, we can see that the maximum AOD_{an} and monthly average of January 2009 were 1.28 and 0.44, respectively. The maximum and monthly average AOD_{an} values for January 2013 were 3.06 and 0.88, respectively, which are much higher than those of 2009, and correspond with the number of days in January 2013 featuring extremely high values. The AOD_{an} of 2013 was 87.9% of the total AOD, while the AOD_{an} of 2009 was 78.9% of the total AOD. This shows that contributions to total aerosols from human activities were higher in January 2013. In this study, the dust and anthropogenic fine fractions (f_{du}, f_{an}) were fixed, but in reality, these values may fluctuate with weather conditions. This suggests there is a certain error for the anthropogenic aerosol optical depth. As there is no chemical composition data for aerosols it is not possible to quantify this error further.

3.2 Analysis of aerosols properties in haze process

In this section, we select two haze events to analyze the relationship between anthropogenic aerosol optical depth and aerosol optical characteristic parameters: January 25 to 29, 2009 and January 24 to 28, 2013 (hereafter referred to as 09 haze and 13 haze events). Fig. 2 shows the AOD_{an} at 440 nm, the total AOD, SSA and the volumes, and aerosol size distributions of the two haze events.

From Fig. 2 (a) (b), we can see that the average AOD of the 2013 haze event is much higher than that of the 2009 haze event. The maximum AOD at 440 nm reaches 3.2 for the 2013 haze event, while that of 2009 is only 1.1. The maximum AOD_{an} of the two haze events are 3.06 and 0.95, respectively. In addition, the 2009 haze event shows a slow increase of AOD, while the AOD of 2013 haze event features large fluctuations. In both haze events, the AOD and AOD_{an} show consistent trends, which suggest that the AOD_{an} makes an overall greater contribution to the total optical thickness during the haze event.

Fig. 2 (c) shows the comparison of the SSA in two pollution events. The SSA of the 2013 haze event gradually increased from 0.83 to 0.90, from a good day to heavy pollution day. This is also in good agreement with the AOD_{an} increase. The larger SSA suggests that the strong scattering may be attributed to anthropogenic aerosols during this period. In the 2009 haze event, the mean SSA was 0.92 in January 25. The SSA was reduced to 0.84 as pollution accumulates and then increases to 0.88. There is also a large difference in the change of the AOD_{an} trend. It may be that coal-fired heating in winter caused an increase of the carbon black content of anthropogenic aerosols, leading to higher absorption and smaller SSA values. It is possible that increases in the volume of aerosol particles may occur through water adsorption (Wang, 2013) as in January 24 to 28, the average relative humidities were 37.6, 46.5, 64.7, 77.7 and 80.9% which correlates with the upward trend of the SSA.

It can be seen that small particles were the main constituent of the bimodal aerosol size distribution during the two haze process (Fig. 2 (d) and Fig. 2 (e)) which is consistent with the research of Yu Xingna (Yu, 2012). During the 09 haze event, on 25 January large particles were the main constituent of the total aerosol size distribution. The amount of small aerosol particles increased continually as the haze event developed. On 27 January, small particles became the main constituent of the total aerosol distribution and gradually increase. During the event AOD_{an} also increased continually. The change in the proportion of small par-

ticles and AOD_{an} during the 2013 haze event occurred on a similar basis to that in 2009. However the average radius of the small particle distribution was larger than that of the 2009 haze event. When the AOD <1.0, the maximum radius value of the small particles is concentrated at 0.11 μm. When the AOD >1.0, the maximum value was concentrated at 0.15—0.43 μm. This is mainly because of the higher relative humidity during the polluted process, which leads to volume growth of the hygroscopic particles (Eck, et al., 2005). During both haze events, the mean peak radius of large particle distribution becomes smaller with an increase of AOD. As an example, over the course of the 2013 haze event, for AOD <1.0, the average peak radius of large particle distribution was centered around 5.06 μm; when AOD >1.0, the average peak radius was about 3.85 μm. A possible reason for this behavior is that when fog and a haze event coincide, the weather system stabilizes, which results in pollutant accumulation.

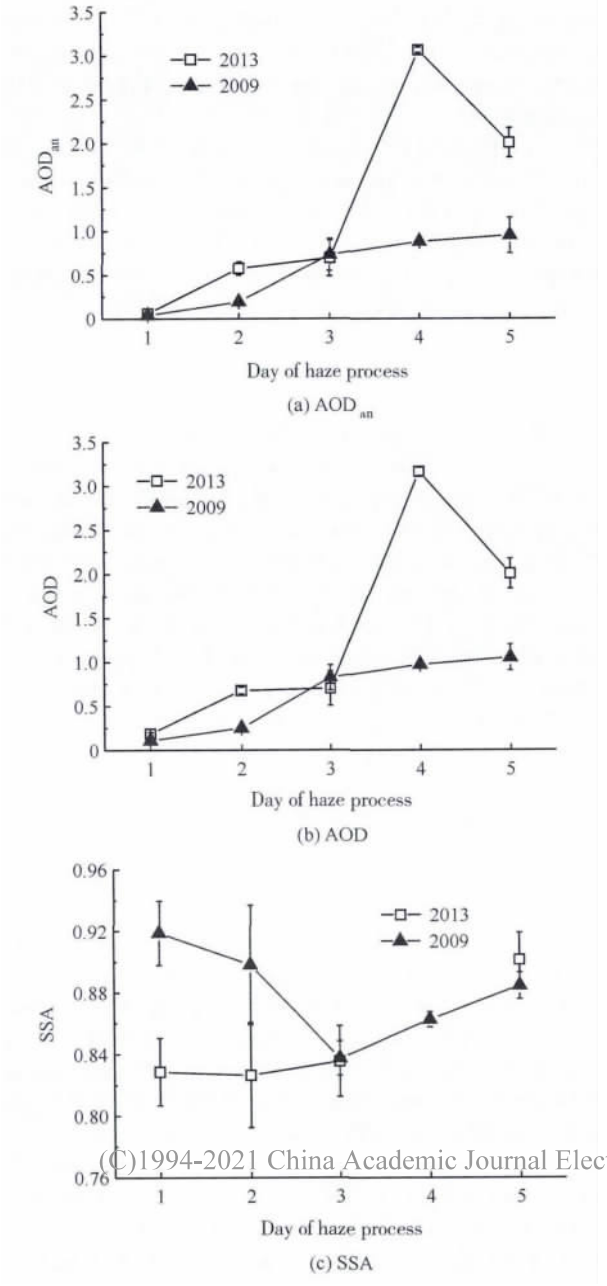

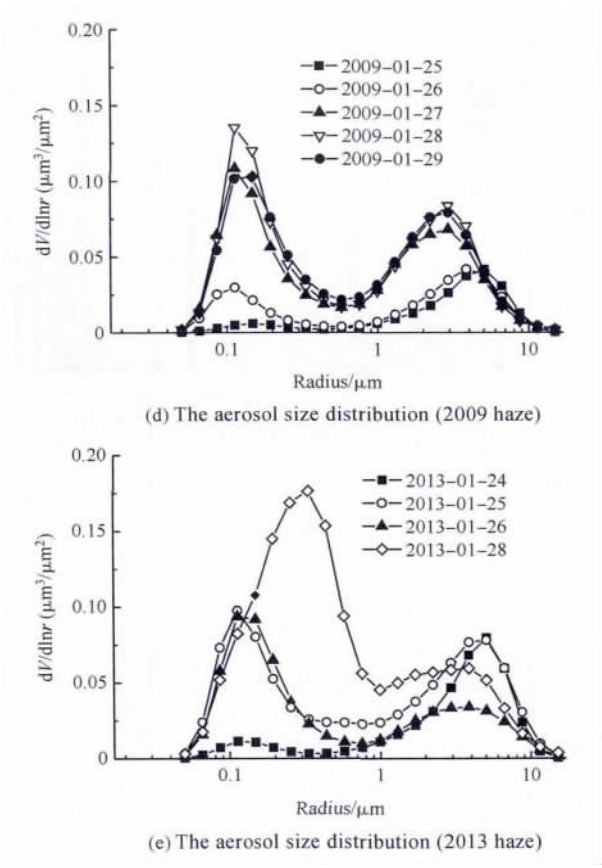

Fig. 2 Contrast changes of aerosols properties in 2009 and 2013 haze process

3.3 Analysis of weather Process in haze pollution

To understand the weather conditions of haze events in Beijing, we analyzed the surface weather charts of region of Huabei at 8:00 pm in January 2009 and January 2013 (Fig. 3 and Fig. 4).

Before January 28, 2009, the surface wind speeds of Beijing were 2—8 m/s in a westerly to northerly direction. The surface wind speed decreases from the January 28 to less than 2 m/s on January 29. At some points the wind speed dropped to 0 m/s. The low wind speeds were the main factor that caused accumulation of regional atmospheric pollutants. From the surface wind

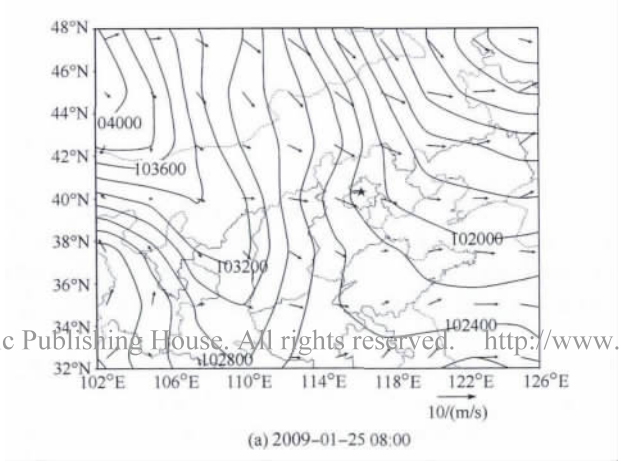

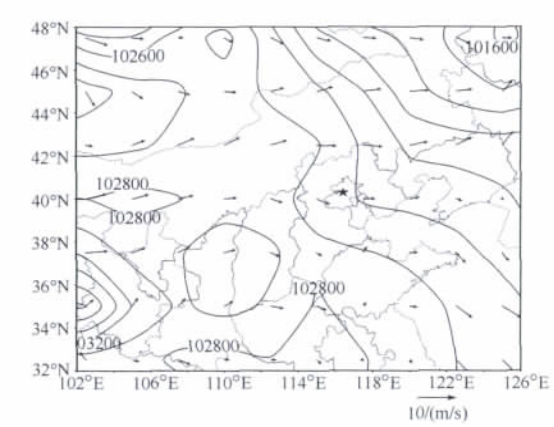

(b) 2009-01-26 08:00

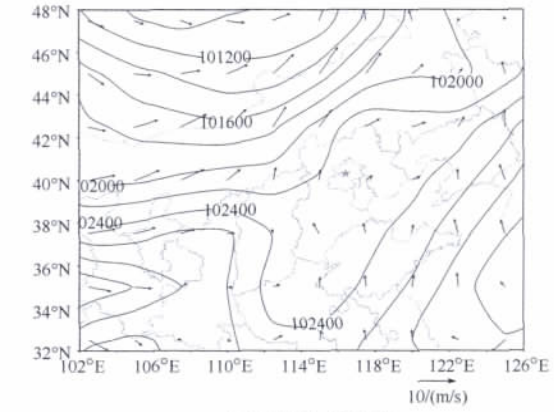

(c) 2009-01-27 08:00

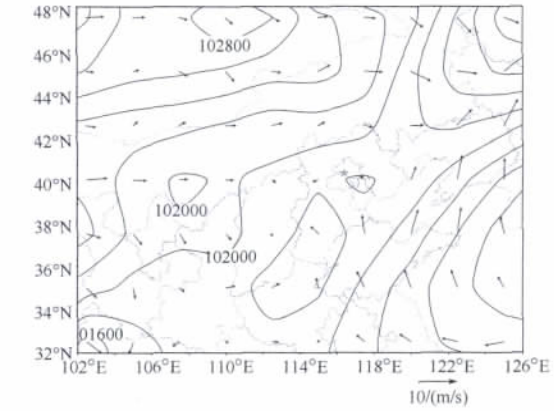

(d) 2009-01-28 08:00

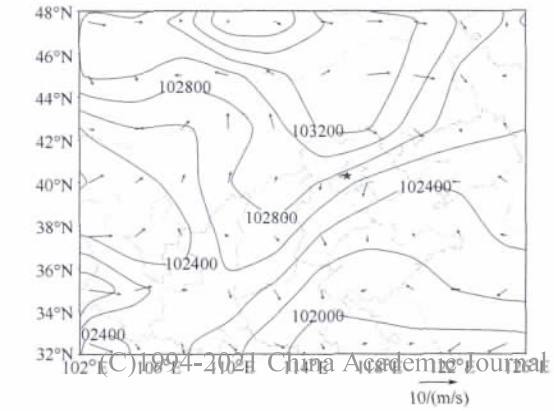

(e) 2009-01-29 08:00

Fig. 3 Chart of 2009-01-25 08:00—2009-01-29 08:00 surface weather

distribution, we can see that during January 25 to 26, 2009, high pressure was located in the northwest and low pressure in the southeast, and the surface wind direction in Beijing was northwesterly, and during January 27 to 29, Beijing was in a region of low pressure with a weak pressure gradient. The atmospheric pollution in Beijing was much more serious because of pollution transported by the southerly wind (Feng, 2008; Xi, 2008).

The surface wind speed was lower than 4 m/s during the entire haze processes of January 2013. From the form of the flow

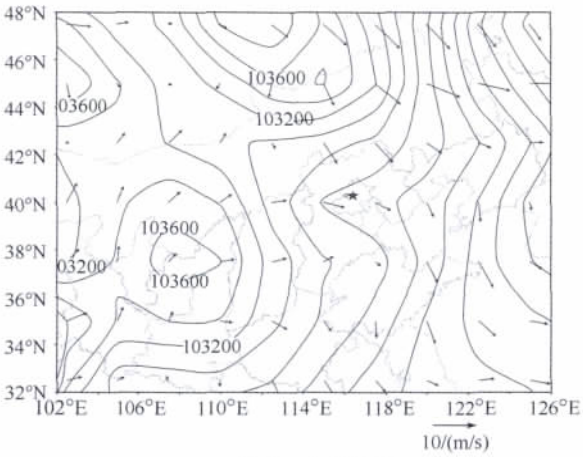

(a) 2013-01-24 08:00

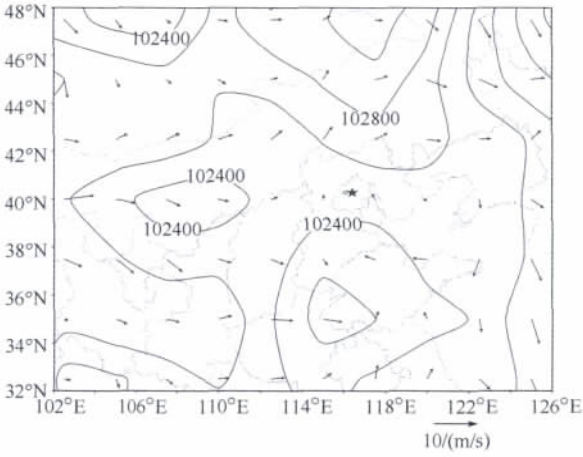

(b) 2013-01-25 08:00

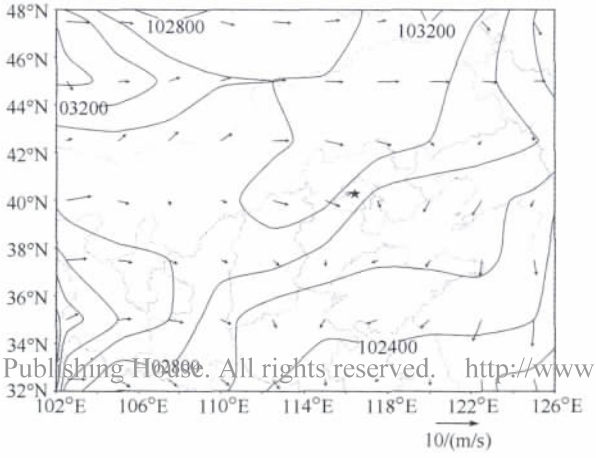

(c) 2013-01-26 08:00

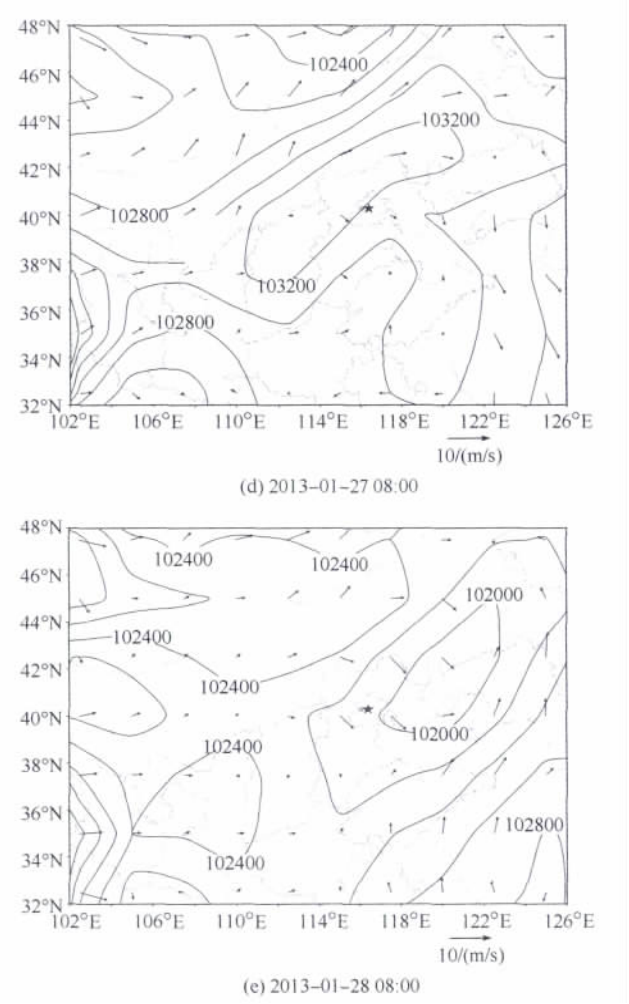

Fig. 4 Chart of January 2013 24 – 28 08 surface weather

field in North China, we can see that on 24 January the surface pressure field was high northwesterly and low northeasterly. D uring January 25 to 26 the bottom of the high-pressure zone and dominant wind direction was northeasterly. On January 27 the pressure field was reduced to a weakened high-pressure zone. During January 27 to 28, the high pressure zone became a low pressure zone and the wind direction changed to southerly. Analysis of the two haze events in 2009 and 2013 show that the s urface wind speed is lower later in the events. It also shows that the degree of pollution in the two haze process was noticably different. Compared with 2009 the local and external sources of the 2013 haze event were enhanced. A possible reason is the i ncrease of anthropogenic emissions around Beijing owing to North China's rapid economic development. The increase in the number of motor vehicles in Beijing is one of factor that may contribute to the increase in local sources. Beijing's air pollution control is influenced by a combination of local sources and sources around Beijing.

4 CONCLUSIONS

In this study, we estimated the AOD_{an} during days of high haze levels using ground-based measurements in Beijing in January 2009 and 2013. We then compared AOD_{an} with retrieved aerosol optical parameters. This work provides a certain reference value to the policy and to understand the effect of h uman activities on haze weather.

However, because of data limitations no further error analysis was possible. We hope to combine ground-based observations with aerosol chemical composition in the near future, so that we can validate our estimation of anthropogenic aerosols in Beijing.

Our main conclusions are as below:

(1) In January 2013, the monthly average AOD at 440 nm was 0.92, greater than 0.52 in January 2009. The value of maximum AOD (3.2) was also higher in 2013 than in 2009 (1.7), showing that atmospheric aerosol levels were higher in January 2013.

(2) The monthly mean AMF (at 440 nm) in January 2013 was 0.87, greater than 0.83 in January 2009. The proportion of days of high anthropogenic aerosol levels (average daily AMF > 0.83) in January 2013 was 86.7% and 62.5% in January 2009.

(3) The monthly mean anthropogenic aerosol optical depths (at 440 nm) in January 2013 and 2009 were 0.88 and 0.44, r espectively. The average proportions of anthropogenic aerosol optical thickness and total optical thickness were 88% and 79%, respectively. This shows that the haze pollution was mainly caused by human activity in January 2013, and was more serious than 2009.

(4) Weather conditions contributed to the heavy haze pollution events in Beijing as a result of the accumulation of local pollution and pollutants transported from southern cities.

REFERENCES

Bellouin N, Boucher O, Haywood J and Reddy M S. 2005. Global estimates of aerosol direct radiative forcing from satellite measurements. Nature, 438(7071): 1138 – 1141 [DOI: 10.1038/nature04348]

Deng X L, Pan D L, He D Y, Mao Z H and Chen Z H. 2009. Anthropogenic and dust aerosol components estimated by satellite data over the China's seas. Acta Oceanologica Sinica, 31(4): 58 – 68

Dubovik O, Smirnov A, Holben B N, King M D, Kaufman Y J, Eck T F and Slutsker I. 2000. Accuracy assessments of aerosol optical properties retrieved from Aerosol Robotic Network (AERONET) Sun and sky radiance measurements. Journal of Geophysical Research, 105 (D8): 9791 – 9806 [DOI: 10.1029/2000JD900040]

Dubovik O, Sinyuk A, Lapyonok T, Holben B N, Mishchenko M, Yang P, Eck T F, Volten H, Muñoz O, Veihelmann B, van der Zande W J, Leon J F, Sorokin M and Slutsker I. 2006. Application of spheroid models to account for aerosol particle nonsphericity in remote sensing of desert dust. Journal of Geophysical Research, 111(D11) [DOI: 10.1029/2005JD006619]

Eck T F, Holben B N, Dubovik O, Smirnov A, Goloub P, Chen H B, Chatenet B, Gomes L, Zhang X Y, Tsay S C, Ji Q, Giles D and Slutsker I. 2005. Columnar aerosol optical properties at AERONET sites in central eastern Asia and aerosol transport to the tropical mid-Pacific. Journal of Geophysical Research, 110(D6) [DOI: 10.1029/2004JD005274]

Goloub P, Li Z, Dubovik O, Blarel L, Podvin T, Jankowiak I, Lecoq R, Lecoq R, Deroo C, Chatenet B, Morel J P, Cuevas E and Ramos R. 2008. PHOTONS/AERONET sunphotometer network overview. Fourteenth International Symposium on Atmospheric and Ocean Optics/Atmospheric Physics, 6936: 9360 – 9360 [DOI: 10.1117/12.783171]

Holben B N, Eck T F, Slutsker I, Tanré D, Buis J P, Setzer A, Vermote E, Reagan J A, Kaufman Y J, Nakajima T, Lavenu F, Jankowiak I and Smirnov A. 1998. AERONET-A federated instrument network and data archive for aerosol characterization. Remote Sensing of Environment, 66(1): 1 – 16 [DOI: 10.1016/S0034 – 4257(98)00031 – 5]

Kaufman Y J, Boucher D, Tanré D, Chin M, Remer L A and Takemura T. 2005a. Aerosol anthropogenic component estimated from satellite data. Geophysical Research Letters, 32(17) [DOI: 10.1029/2005GL023125]

Kaufman Y J, Koren I, Remer L A, Tanré D, Ginoux P and Fan S. 2005b. Dust transport and deposition observed from the Terra-Moderate Resolution Imaging Spectroradiometer (MODIS) spacecraft over the Atlantic Ocean. Journal of Geophysical Research, 110(D10) [DOI: 10.1029/2003JD004436]

Li Z Q, Gu X, Wang L, Li D, Li K, Dubovik O, Schuster G, Goloub P, Zhang Y, Li L, Xie Y, Ma Y and Xu H. 2013. Aerosol physical and chemical properties retrieved from ground-based remote sensing measurements during heavy haze days in Beijing winter. Atmospheric Chemistry and Physics Discussions, 13(2): 5091 – 5122 [DOI: 10.5194/acpd – 13 – 5091 – 2013]

Ma F M, Gao Q X, Zhou S Q, Su F Q, Kang N and Sun J. 2008. The simulation and analysis of a typical pollution event around Beijing. Research of Environmental Sciences, 21(1): 30 – 36

O'Neill N T, Eck T F, Smirnov A, Holben B N and Thulasiraman S. 2003. Spectral discrimination of coarse and fine mode optical depth. Journal of Geophysical Research, 108(D17) [doi]

Ren X Y, Ji D S, Wang Y S, Hu B and Sun Y. 2008. The characteristics of the concentrations of fine particles and their composition in Beijing. Geo-Information Science, 10(4): 426 – 430

Schuster G L, Lin B and Dubovik O. 2009. Remote sensing of aerosol water uptake. Geophysical Research Letters, 36(L03814) [DOI: 10.1029/2008GL036576]

Sun J R and Liu Y. 2008a. Possible effect of aerosols over China on East Asian Summer Monsoon (I): Sulfate aerosols. Advances in Climate Change Research, 4(2): 111 – 116

Sun J R and Liu Y. 2008b. Possible effects of aerosols over China on East Asian Summer Monsoon (II): Black carbon and its joint effects with sulfate aerosols. Advances in Climate Change Research, 4(3): 161 – 166

Tanré D, Kaufman Y J, Holben B N, Chatenet B, Karnieli A, Lavenu F, Blarel L, Dubovik O, Remer L A and Smirnov A. 2001. Climatology of dust aerosol size distribution and optical properties derived from remotely sensed data in the solar spectrum. Journal of Geophysical Research, 106(D16): 18205 – 18217 [DOI: 10.1029/2000JD900663]

Wang L, Li Z Q, Ma Y, Li L and Wei P. 2013. Retrieval of aerosol chemical composition from ground-based remote sensing data of sun-sky radiometers during Haze Days in Beijing Winter. Journal of Remote Sensing, 17(4): 944 – 958 [DOI: 10.11834/jrs.20133059]

Wang Y, Che H Z, Ma J Z, Wang Q, Shi G Y, Chen H B, Goloub P and Hao X J. 2009. Aerosol radiative forcing under clear, hazy, foggy, and dusty weather conditions over Beijing, China. Geophysical Research Letters, 36(6) [DOI: 10.1029/2009gl037181]

Wu D, Deng XJ, Bi XY. 2007. Distinguishing of fog or haze and the operational criteria for observation, forecasting and early warning of haze in urban areas of Guangdong, Hong Kong and Macau. Guangdong Meteorology, 29(2): 5 – 28

Yan P, Liu G Q, Zhou X J, Wang J L, Tang J, Liu Q, Wang Z F and Zhou H G. 2010. Characteristics of aerosol optical properties during haze and fog episodes at Shangdianzi in Northern China. Journal of Applied Meteorological Science, 21(3): 257 – 265

Yu X N, Li X M, Deng Z G, De Q Y and Yuan S. 2012. Optical properties of aerosol during haze-fog episodes in Beijing. Environmental Science, 33(4): 1057 – 1062

Zhang Y and Li Z Q. 2013. Estimation of $PM_{2.5}$ from fine-mode aerosol optical depth. Journal of Remote Sensing, 17(4): 929 – 943 [DOI: 10.11834/jrs.20133063]

China Meteorological Administration. 2010. Observation and forecasting levels of haze. Beijing: China Meteorological Press

北京区域冬季灰霾过程中人为气溶胶光学厚度估算

王堰[1]，谢一凇[1,2]，李正强[1]，李东辉[1,2]，李凯涛[1,2]

1. 中国科学院 遥感与数字地球研究所 国家环境保护卫星遥感重点实验室，北京 100101;
2. 中国科学院大学，北京 100049

摘 要: 本文使用北京地区不同时期(2009 年 1 月和 2013 年 1 月)的地基气溶胶观测资料,估算了灰霾天气的人为气溶胶光学厚度,在此基础上结合气溶胶光学参数进行了对比分析。结果表明:(1)2013 年 1 月人为气溶胶光学厚度(440 nm)较 2009 年 1 月有所增加,月平均值分别为 0.88 和 0.44;(2)2013 年 1 月灰霾污染中人为气溶胶占主导天数比例是 86.7%,高于 2009 年 1 月的 62.5%;(3)2013 年 1 月人为成分在气溶胶光学厚度(440 nm)中的贡献平均达 88%,说明灰霾污染主要是由人为气溶胶造成的;(4)本文所选取的两次灰霾天气,都是由北京本地污染物堆积和南部周边城市污染物外源的输入共同作用造成的。

关键词: 人为气溶胶光学厚度,灰霾,气溶胶细模态比例,地基气溶胶

中图分类号: TP701 **文献标志码**: A

引用格式: 王堰,谢一凇,李正强,李东辉,李凯涛. 2013. 北京区域冬季灰霾过程中人为气溶胶光学厚度估算. 遥感学报,17(4): 993 – 1007

Wang Y, Xie Y S, Li Z Q, Li D H and Li K T. 2013. Anthropogenic aerosol optical depth during days of high haze levels in the Beijing winter. Journal of Remote Sensing, 17(4): 993 – 1007 [DOI: 10.11834/jrs.20133071]

1 引 言

灰霾污染由于其在公众健康、交通安全、环境问题等方面的重大危害,已经成为公众关注度很高的话题。北京是华北地区最大的城市,人口和机动车数量在近 20 年内快速增长,大量人为排放的污染物长期影响北京区域的大气环境。从 2008 年北京奥运会之后,北京区域空气质量有所下降,近几年秋冬季频频出现严重的灰霾污染事件,如 2011 年 2 月和 2012 年 2 月出现的灰霾天气(Li 等,2013)。特别是 2013 年 1 月爆发的灰霾持续污染过程,据统计,这个月仅有 5 天达到无灰霾的环保标准。许多学者对城市灰霾的气溶胶光学特性进行了相关研究(严鹏 等,2010; 于兴娜 等,2012; Wang 等,2009),但关于灰霾中人为气溶胶光学厚度的研究还比较少。

根据气溶胶来源不同,可大体分为自然气溶胶和人为气溶胶,自然气溶胶主要包括沙尘和海盐类等较大颗粒的气溶胶,而人为气溶胶主要是人为活动排放的尺寸较小的颗粒物,包括硫酸盐、硝酸盐、黑碳、有机碳气溶胶等。关于人为气溶胶的辐射强迫作用和气候效应已经有许多研究成果(孙家仁和刘昱,2008a,2008b)。

目前利用遥感技术区分自然和人为气溶胶主要是通过气溶胶细模态(光学厚度)比例 AMF(Accumulation Mode Fraction),下文简称为细模态比例,来实现的(Bellouin 等,2005)。AMF 定义为细模态气溶胶光学厚度在总光学厚度中所占的比例(O'Neill 等,2003)。目前一般把 AMF > 0.83 的情况归类为人为气溶胶,而 AMF < 0.35 则归类为自然气溶胶(Bellouin等,2005)。Kaufman 等人(2005b)提出了基于 MODIS 卫星遥感的人为气溶胶估算方法,将气溶胶分为沙尘气溶胶,海盐气溶胶以及人为气溶胶。邓学良等人(2009)将该方法应用到中国海域,进行了人为气溶胶和沙尘气溶胶时空分布的研究。

本文将该方法推广到地基气溶胶遥感领域,利

收稿日期: 2013-03-26; **修订日期**: 2013-05-14; **优先数字出版日期**: 2013-05-21

基金项目: 国家重大科学研究计划(编号: 2010CB950800,2010CB950801); 中国科学院战略性先导科技专项(编号: XDA05100202)

第一作者简介: 王堰(1974—),女,博士,现从事大气气溶胶及其辐射效应研究。E-mail: wylf369@sina.com

通信作者简介: 李正强(1977—),男,研究员,主要从事大气环境遥感研究。E-mail: lizq@irsa.ac.cn

用地基观测数据,估算了 2013 年 1 月份灰霾污染过程中的人为气溶胶光学厚度,并同时计算了 2009 年 1 月份结果作为对比,结合气溶胶光学特性参数,对其特征展开分析。

2 数据与研究方法

2.1 观测数据

本文利用的是地基气溶胶观测网 AERONET (AErosol RObotic NETwork) 北京站点(经纬度 39.98°N,116.38°E,海拔 92 m) 2009 年 1 月和 2013 年 1 月的观测数据。AERONET 是美国 NASA(Holben 等,1998) 与法国 PHOTONS(Goloub 等,2008) 等机构联合发起的气溶胶地基监测网络,致力于监测全球主要区域的气溶胶光学特性。AERONET 所应用的观测仪器是法国 CIMEL 公司制造的太阳-天空辐射计 CE318,可以通过太阳直射光和天空光两种观测模式进行紫外、可见光和近红外的多角度持续观测,并基于遥感方法获得大气气溶胶特性(Schuster 等,2009; Dubovik 等,2000,2006)。本文中用到的数据产品包括气溶胶光学厚度 AOD、AMF,以及单次散射反照率 SSA、粒子谱分布等气溶胶光学参数。

根据空气质量指数 AQI (Air Quality Index) (2013 年前为 API) 可以区分清洁天气和污染天气,通常 AQI≤100 时空气质量为优或良,反之为污染。灰霾主要监测的指标有湿度、能见度、悬浮颗粒的大小等(吴兑,2007; 中国气象局,2010)。按照此标准结合气象数据选取了 2009 年和 2013 年灰霾污染过程。表 1 给出了两个不同时期的 1 月份天气污染状况。2009 年 1 月份,北京良好天气为 24 天,占一个月的 77.4%; 中度污染以上的天气为 0 天。而 2013 年 1 月份,良好天气为 10 天,仅占一个月的 32.2%,中度污染和中度以上的污染天气为 16 d,占一个月的 51.6%。因此选择这两个月对比分析气溶胶光学性质和人为气溶胶的差别,是比较具有代表性的。

表 1 2009、2013 年 1 月份天气污染状况统计 /d

年	优	良	轻微污染	>轻微污染
2009	5	19	7	0
2013	3	7	6	15

2.2 研究方法

本文使用 Kaufman 等人(2005a,2005b) 提出的算法,将其推广到地基遥感观测中,得到北京地区人为气溶胶光学厚度的计算结果。自然和人为气溶胶中细粒子和粗粒子所占的比例不同,如城市工业污染和生物质燃烧(绝大部分是人为来源) 主要是细粒子气溶胶,而沙尘和海盐(自然源) 则主要是粗粒子气溶胶(Tanré 等,2001),应用遥感技术可以区分并提取这两种模态的气溶胶光学厚度。为了从总气溶胶光学厚度中计算得到人为气溶胶光学厚度,须作如下假设(Kaufman 等,2005b; 邓学良等,2009):

(1) 假设气溶胶分为人为源和自然源两种,其中自然源气溶胶只包括沙尘类和海盐类气溶胶,不包括自然条件下燃烧产生的气溶胶,而人为源气溶胶中不包括人类活动产生的沙尘和海盐。

(2) 假设对于某一种气溶胶类型(人为、沙尘、海盐),AMF 是固定的。

根据以上的假设,可以将波长 λ 处总气溶胶光学厚度 AOD(λ) 写成下面的形式:

$$\tau(\lambda) = \tau_{an}(\lambda) + \tau_{du}(\lambda) + \tau_{ma}(\lambda) \quad (1)$$

式中,右边 3 项依次为波长 λ 处的人为气溶胶光学厚度、沙尘气溶胶光学厚度和海盐气溶胶光学厚度。气溶胶细粒子光学厚度 AOD_f 可以通过 AMF 计算得到:

$$\tau_f(\lambda) = \tau(\lambda) \cdot AMF \quad (2)$$

式中,AMF 可来自于太阳-天空辐射计观测。对于细粒子光学厚度来说,也可进一步根据其来源分为人为、沙尘和海盐 3 类:

$$\tau_f(\lambda) = f_{an}\tau_{an}(\lambda) + f_{du}\tau_{du}(\lambda) + f_{ma}\tau_{ma}(\lambda) \quad (3)$$

式中,f_{an}、f_{du}与 f_{ma}分别是人为气溶胶、沙尘气溶胶和海盐气溶胶中细粒子权重,对于相同种类气溶胶是常量(Kaufman 等,2005b)。

北京区域冬季主要盛行风向是西北风,从东部和东南部海上吹来的海盐气溶胶粒子极少,因此可以进一步假设海盐气溶胶光学厚度为 0,即 $AOD_{ma}(\lambda)$ 为 0。由于海盐气溶胶属于自然气溶胶,因此该假设对人为气溶胶的估算影响不大。

基于上述分析,联合式(1)—式(3),只要给出 f_{an}与 f_{du},即可求出人为气溶胶和沙尘气溶胶的光学厚度。Kaufman 等人(2005b) 分别计算了典型区域的人为气溶胶和沙尘气溶胶细粒子比例(0.92 ± 0.03 和 0.51 ± 0.03) 作为式(3) 中的 f_{an}与 f_{du}。

获取 AMF 参数主要有两种方法: 第 1 种方法是基于气溶胶体积谱分布利用 Mie 散射理论直接计算

获得 AMF 参数(AERONET [2013-02-17] http://aeronet.gsfc.nasa.gov/cgi-bin/type_piece_of_map_opera_v2_inv2);第 2 种方法是利用光谱退卷积方法求解 500nm 的 AMF(O'Neill 等 2001,2003;张莹 等,2013)。本文利用第 1 种方法获取 440 nm 的 AMF 值。

为验证该权重值能否应用于本文,分别选择北京严重灰霾污染天气(2010-10-09)和沙尘暴天气(2004-04-17),用实测的气溶胶粒子谱分布数据通过米散射计算,得到北京区域的典型的灰霾和沙尘天气状况下的 f_{an} 和 f_{du}。

2010 年 10 月 09 日在北京理工大学利用 APS3321 仪器得实测地面气溶胶粒子谱分布,得到 f_{an} 和 0.92(Kaufman,2005b),较为接近;而 f_{du} 同 0.50(Kaufman,2005b)较为一致,因此选取这两个数值作为对人为气溶胶的估算。

3 结果与分析

3.1 灰霾污染期间人为气溶胶光学厚度

图 1 显示了 2009 年 1 月与 2013 年 1 月 440 nm 处的 AOD、AMF 和 AOD_{an} 随时间的变化情况。从图 1(a)中可以看出,2013 年 1 月份 AOD 整体水平高于 2009 年 1 月,AOD 均值分别为 0.92 和 0.52,2013 年 1 月份比 2009 年 1 月份高 77%。另外 2009 年 1 月份只有 2 天 AOD 大于 1.0,而 2013 年 1 月有 4 天,且 AOD 峰值也达到 3.2,远高于 2009 年 1 月份的 AOD 峰值 1.7,说明 2013 年 1 月份大气气溶胶浓度高。

AMF 作为判断人为气溶胶的主要参数,在 2009 年 1 月、2013 年 1 月这两个时期的数值上也有明显差异,如图 1(b)所示。2009 年 1 月份 AMF 的最小值为 0.37,最大值为 0.93,月平均值为 0.83;而 2013 年 1 月份 AMF 的最小值为 0.64,最大值为 0.96,月平均值为 0.87,明显高于 2009 年。从图 1(b)可以看出,2009 年 1 月 AMF 值主要在 0.8 附近持续波动,1 月 23 日—25 日有一次明显的下降过程;而 2013 年 1 月的 AMF 值则基本保持在 0.8 以上,只有两天小幅下降到 0.6—0.7(1 月 8 日与 24 日)。根据 Bellouin(2005)的判断方法,2009 年 1 月份的人为气溶胶天气(日平均值 AMF > 0.83)天数为 15 d,占统计天数的 62.5%,自然气溶胶天气(日平均 AMF 值 < 0.35)占 4.2%,其他是两者的混合天气,占 33.3%;2013 年 1 月份,人为气溶胶天气占 86.7%,混合天气为 13.3%,没有自然气溶胶天气。

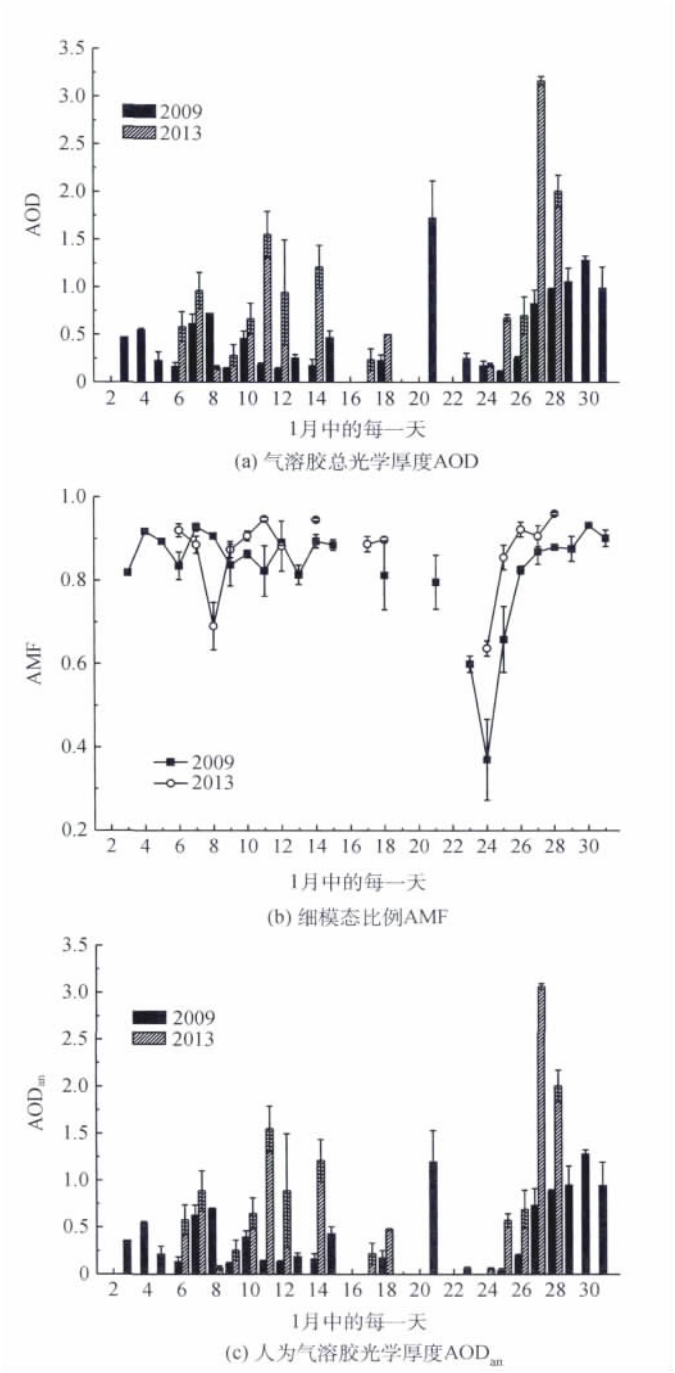

图 1 2009 年 1 月与 2013 年 1 月日平均 AOD、AMF 和 AOD_{an}

基于 2.2 节介绍的方法,计算了人为气溶胶光学厚度 AOD_{an}。从图 1(c)可以看出,AOD_{an} 与 AOD、AMF 同步性较好,AMF 值明显下降的过程对应较低的人为气溶胶光学厚度(如 2009 年 1 月 18、23 日—25 日和 2013 年 1 月 8 日、24 日)。对比 2009 年和 2013 年 1 月份 AOD_{an} 计算结果可以看出,2009 年 1 月份人为气溶胶光学厚度日均值最大为 1.28,月平

均值为0.44,而2013年1月份人为气溶胶光学厚度最大为3.06,月平均值为0.88,平均水平较高,并且从持续天数到极值都明显高于2009年1月份。2013年1月人为气溶胶光学厚度在总光学厚度中的平均贡献高达87.9%,而2009年1月份这一比例为78.9%,说明北京区域冬季气溶胶光学厚度主要受人为气溶胶光学厚度的影响。在气溶胶类型的细粒子比例上,本文采用固定值,而实际情况中不同的天气和时间其大小是变化的,因此对人为气溶胶光学厚度大小的估算上存在着一定误差。因为没有对应时期气溶胶的化学成分观测结果分析,还不能对研究结果做进一步的误差分析。

3.2 灰霾过程中气溶胶特性分析

本节分别选择2009年1月25日—29日和2013年1月24日—28日两个灰霾天气过程(下文分别写为2009灰霾和2013灰霾)来对比分析人为气溶胶光学厚度与气溶胶光学特性参数的关系。图2显示了两次灰霾过程中440 nm处的AOD_{an}、AOD、单次散射反照率(SSA)及气溶胶粒子体积谱分布。

从图2(a)(b)可以看出,2013灰霾过程中AOD平均水平较高,440 nm处AOD最大为3.2,而2009灰霾过程中只有1.1,对应的AOD_{an}最大值分别为3.06和0.95。另外,相比2009灰霾过程中AOD的缓慢增大,2013灰霾过程AOD呈现出较大的波动。两次灰霾过程中AOD和AOD_{an}均表现一致性较高的变化趋势,进一步说明了灰霾过程中人为气溶胶光学厚度对总光学厚度的最大贡献。

图2(c)显示了两次污染过程中SSA的对比,2013灰霾过程中SSA从晴好天气的0.83逐渐增加到污染天气的0.90,且与AOD_{an}增加趋势有较好的一致性,较大的SSA说明在此过程中人为气溶胶有较强的散射性质。2009灰霾过程中开始SSA均值为0.92,随着污染物的堆积先降低到0.84,然后再上升到0.88,与AOD_{an}变化趋势有较大差异,这可能是因为冬季燃煤取暖造成人为气溶胶中黑碳成分增加,吸收作用增强,导致SSA有明显的下降,之后气溶胶粒子由于吸湿增长体积增大,颗粒物中水分含量增加(王玲 等,2013),(1月24日—28日日平均相对湿度分别为37.6%,46.5%,64.7%,77.7%,80.9%)导致SSA出现上升趋势。

图2(d)(e)显示了两次灰霾污染的气溶胶体积谱分布,可以看出,北京区域灰霾期间气溶胶主要以细粒子为主,气溶胶体积谱分布表现为双峰模态,与于兴娜等(2012)的研究结果一致。2009灰霾过程初始阶段(2009年1月25日)粒子谱分布以粗模态为主,在发展过程中细模态气溶胶持续增长,1月27日成为主要模态,并继续增长;相应的,在这一过程中AOD_{an}持续增大。2013灰霾过程也有类似变化,粒子谱分布中细模态体积逐渐增大,AOD_{an}总体上也保持增大趋势。需要注意的是,不同于2009灰霾过程,2013灰霾过程粒子谱分布出现了细模态平均峰值半径增大的情况。具体来说,当AOD<1.0时,细粒子的平均峰值半径主要集中在0.11 μm;AOD>1.0时,平均峰值半径增大到0.15—0.43 μm,这主要是由于灰霾天气期间较高的相对湿度导致粒子吸湿增长体积变大的结果(Eck 等,2005)。在两次灰霾过程中,粗模态的平均峰值半径随着AOD增大都表现出减小趋势,例如在2013灰霾过程中当AOD<1.0时,粗模态的平均峰值半径主要集中在5.06 μm左右;当AOD>1.0,平均峰值半径为3.85 μm左右。可能的原因是在雾霾天气时,天气系统稳定,造成污染物的累积。

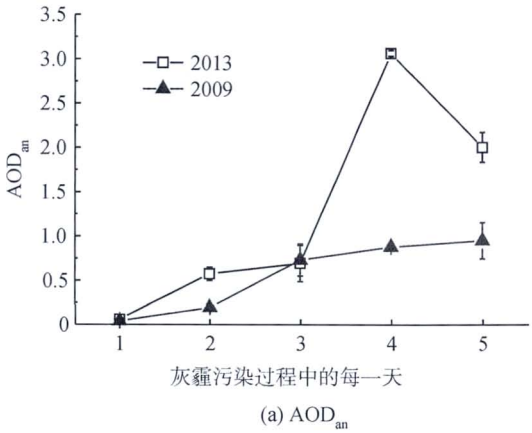

(a) AOD_{an}

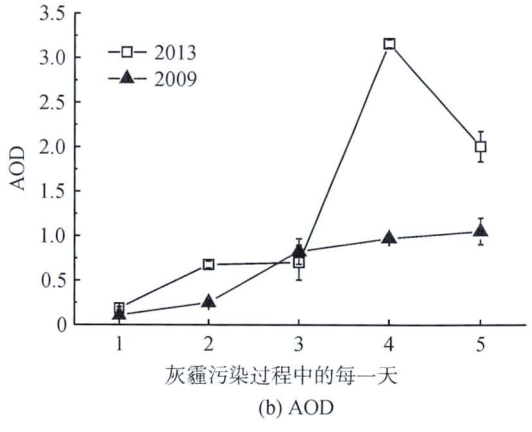

(b) AOD

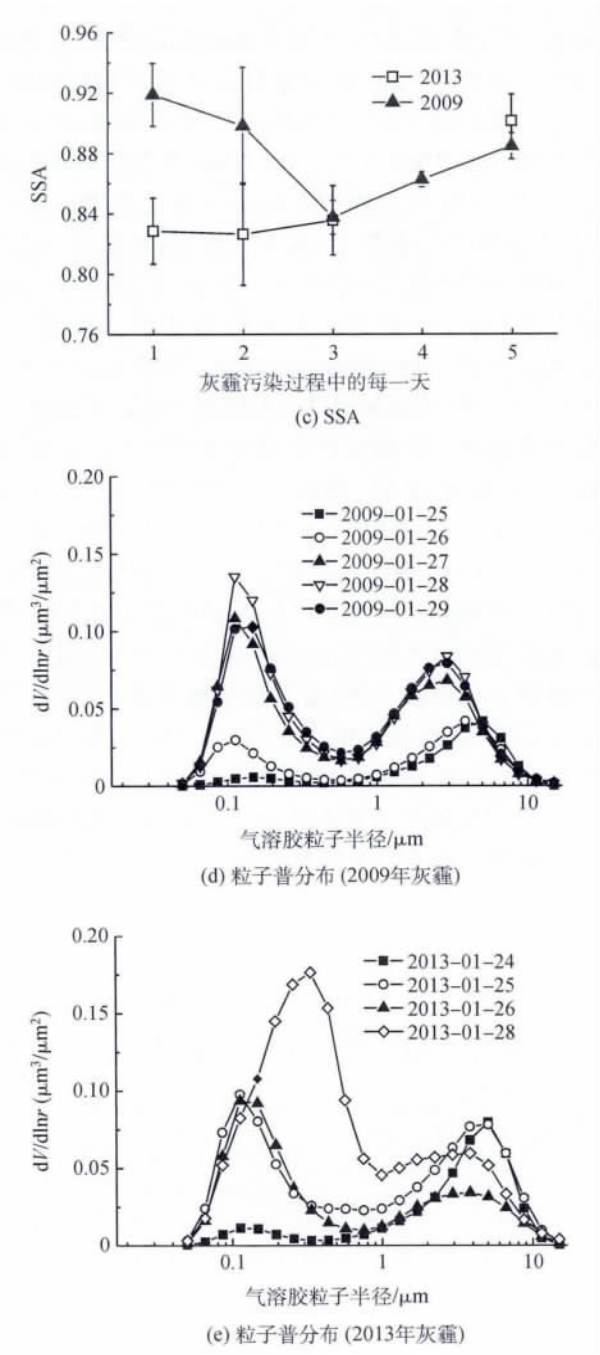

图 2 2009 年和 2013 年灰霾过程中气溶胶光学性质的对比变化

3.3 灰霾污染天气过程分析

为了解北京灰霾过程期间的天气概况,分析了 2009 和 2013 年灰霾过程中整个华北地区 08 时地面天气图(图 3、图 4),从地面天气图上可以看到北京地区地面流场的情况。

2009 年灰霾过程期间,在 28 日之前北京的风速为 2—8 m/s,风向以偏西到偏北风为主;从 28 日风速减小,29 日风速小于 2 m/s,部分时间为静风,这是造成局地污染物堆积的最主要原因。从流场来看:25 日—26 日,地面形势西北高东北低,近地面为西北风,27 日—29 日处于低压带,且气压场较弱,受偏南气流影响,北京受到来自南部污染的输送(马锋敏 等,2008;任希岩,2008),这也使得北京地区污染进一步加强。

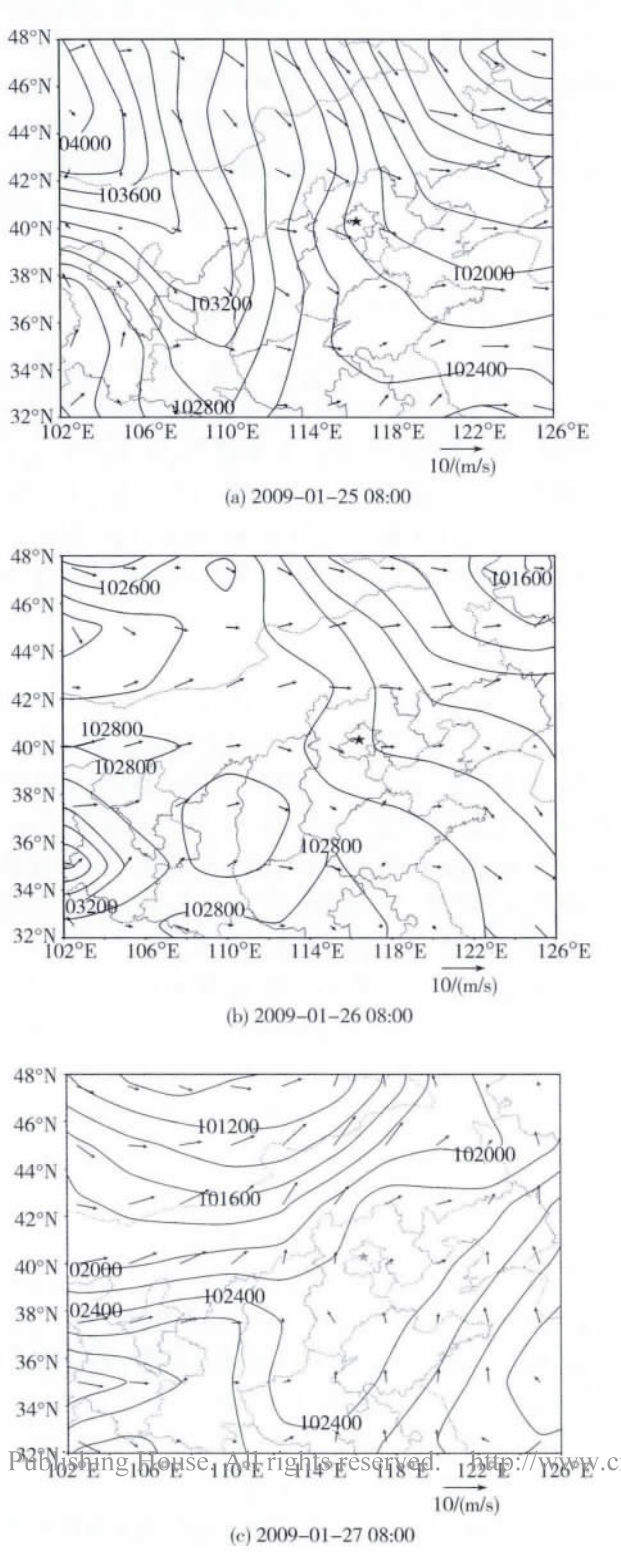

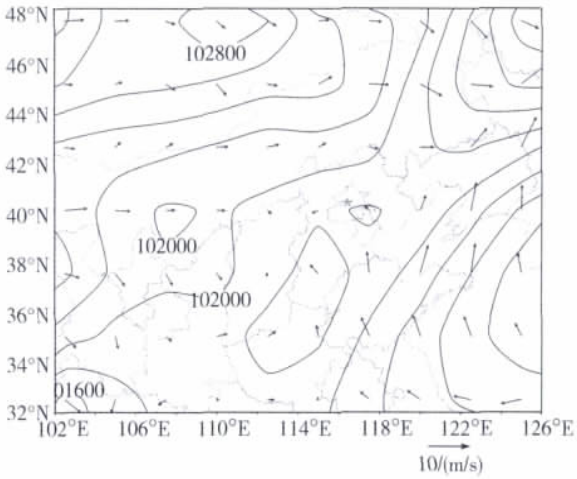

(d) 2009-01-28 08:00

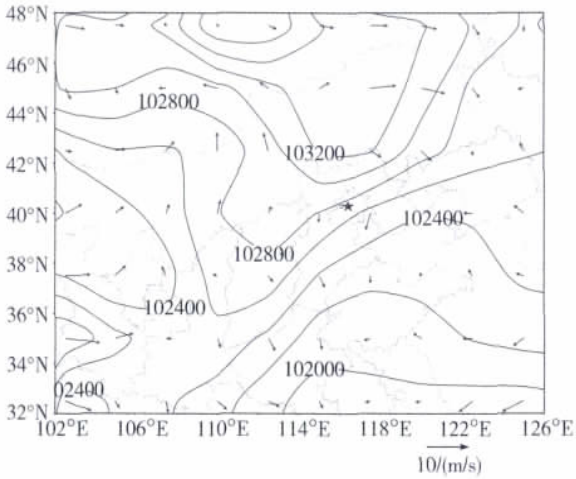

(e) 2009-01-29 08:00

图 3　2009 年 1 月 25 日—29 日 08 时地面天气

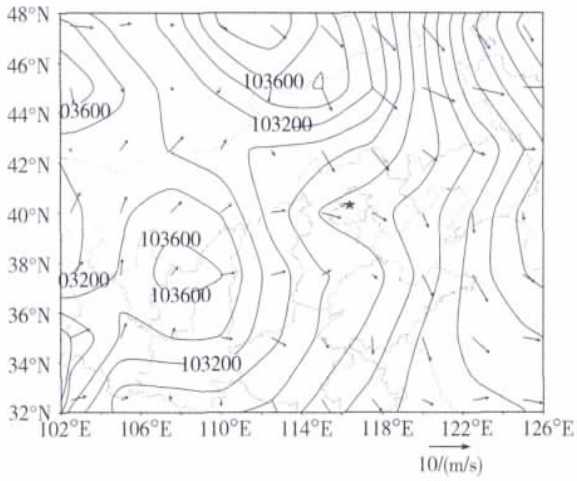

(a) 2013-01-24 08:00

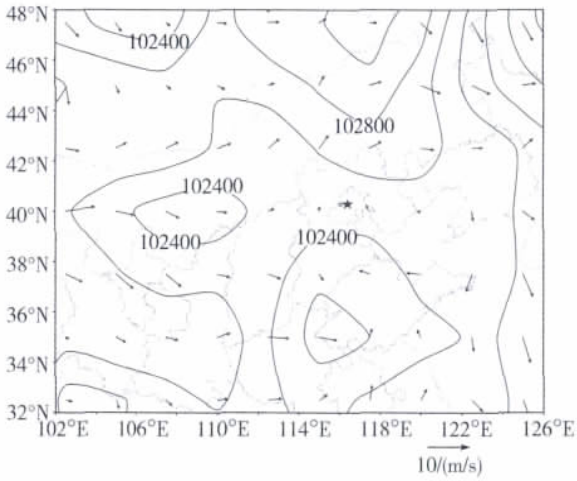

(b) 2013-01-25 08:00

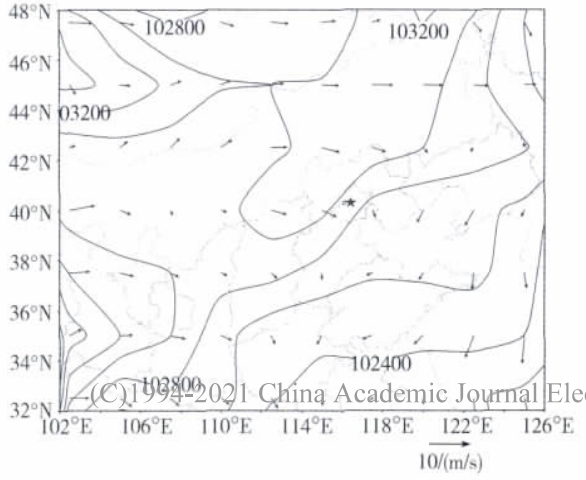

(c) 2013-01-26 08:00

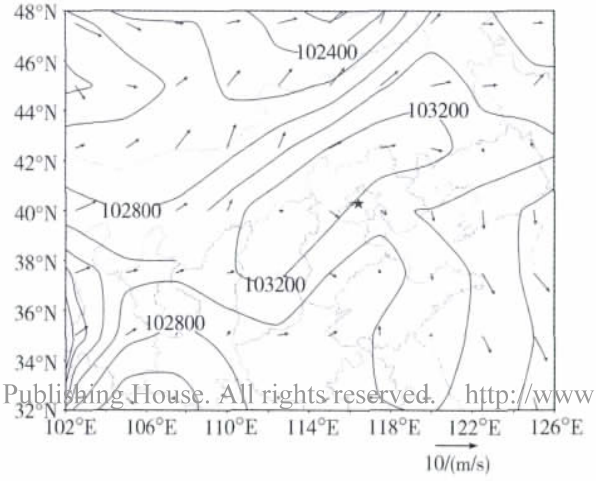

(d) 2013-01-27 08:00

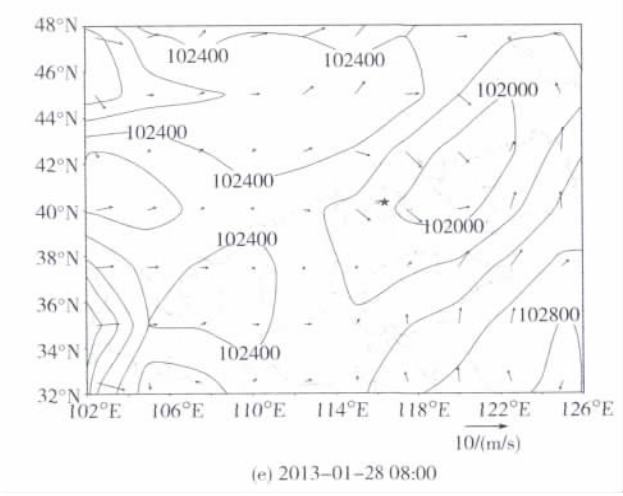

图 4 2013 年 1 月 24 日—28 日 08 时地面天气

2013 年的灰霾过程,整个灰霾过程期间北京区域地面风速都小于 4 m/s。从整个华北地区流场形式来看:24 日西北高东北低的地面气压场形势,25 日—26 日处于高压底部的高压带,主导风向为东北;27 日气压场减弱,为弱高压带,27 日后转为弱低压带,一直到 28 日均处于弱低压带,风向为偏南风。从以上的分析来看针对 2009 年和 2013 年这两次灰霾过程,过程期间北京地面风速较小,而在过程后期都有来自于南部的气流输送。从上面分析可知两次污染程度差别比较明显,这说明了造成 2013 年灰霾过程的北京区域局地源和外来源较 2009 年增强所致。可能的原因是近几年华北地区经济的快速发展在一定程度上增加了北京周边人为源的排放。北京机动车数量的增加是造成局地源增加的一个原因,因此在治理北京空气污染同时也要考虑周边的地区的环境治理。

4 结 论

本文利用地基气溶胶观测网 AERONET 数据,估算了北京区域 2009 年 1 月份和 2013 年 1 月份人为气溶胶光学厚度,并结合其他气溶胶光学参数进行对比分析,了解人为活动对灰霾天气的贡献程度以及相关政策具有一定的参考价值。但是由于资料的限制还未能对结果做进一步的误差分析,希望以后能够结合地基观测的气溶胶化学成分组成,对估算得到人为气溶胶进行验证和误差分析。

主要得到以下结论:

(1) 2013 年 1 月份 440 nm 处的月平均气溶胶光学厚度为 0.92,大于 2009 年 1 月份的月平均气溶胶光学厚度值 0.52,AOD 最大值 3.2 也高于 2009 年的 AOD 值 1.7,显示出 2013 年 1 月份大气气溶胶含量较高。

(2) 2013 年 1 月份 AMF 月均值(440 nm)为 0.87,大于参照组 2009 年 1 月的 AMF 月均值(440 nm) 0.83,而从人为气溶胶天数(日平均 AMF 大于 0.83)所占比例来看,2013 年 1 月的 86.7% 也大于 2009 年 1 月的 62.5%。

(3) 2013 年 1 月与 2009 年 1 月人为气溶胶光学厚度(440 nm)月均值分别为 0.88 和 0.44。相应的人为气溶胶光学厚度占总光学厚度的平均比例为 88% 和 79%。这说明了灰霾污染主要是由人为造成,并且 2013 年 1 月的污染情况更为严重。

(4) 北京地区强灰霾天气的过程,往往是北京本地污染物的堆积以及南部周边城市染物的输送共同作用的结果。

参考文献(References)

Bellouin N, Boucher O, Haywood J and Reddy M S. 2005. Global estimates of aerosol direct radiative forcing from satellite measurements. Nature, 438(7071): 1138 – 1141 [DOI: 10.1038/nature04348]

邓学良, 潘德炉, 何冬燕, 毛志华, 陈正华. 2009. 卫星遥感中国海域人为和沙尘气溶胶时空分布的研究. 海洋学报, 31(4): 58 – 68

Dubovik O, Smirnov A, Holben B N, King M D, Kaufman Y J, Eck T F and Slutsker I. 2000. Accuracy assessments of aerosol optical properties retrieved from Aerosol Robotic Network (AERONET) Sun and sky radiance measurements. Journal of Geophysical Research, 105(D8): 9791 – 9806 [DOI: 10.1029/2000JD900040]

Dubovik O, Sinyuk A, Lapyonok T, Holben B N, Mishchenko M, Yang P, Eck T F, Volten H, Muñoz O, Veihelmann B, van der Zande W J, Leon J F, Sorokin M and Slutsker I. 2006. Application of spheroid models to account for aerosol particle nonsphericity in remote sensing of desert dust. Journal of Geophysical Research, 111(D11) [DOI: 10.1029/2005JD006619]

Eck T F, Holben B N, Dubovik O, Smirnov A, Goloub P, Chen H B, Chatenet B, Gomes L, Zhang X Y, Tsay S C, Ji Q, Giles D and Slutsker I. 2005. Columnar aerosol optical properties at AERONET sites in central eastern Asia and aerosol transport to the tropical mid-Pacific. Journal of Geophysical Research, 110(D6) [DOI: 10.1029/2004JD005274]

Goloub P, Li Z, Dubovik O, Blarel L, Podvin T, Jankowiak I, Lecoq R, Lecoq R, Deroo C, Chatenet B, Morel J P, Cuevas E and Ramos R. 2008. PHOTONS/AERONET sunphotometer network overview. Fourteenth International Symposium on Atmospheric and Ocean Optics/Atmospheric Physics, 6936: 9360 – 9360 [DOI: 10.1117/12.783171]

Holben B N, Eck T F, Slutsker I, Tanré D, Buis J P, Setzer A, Vermote E, Reagan J A, Kaufman Y J, Nakajima T, Lavenu F, Jankowiak I and Smirnov A. 1998. AERONET-A federated instru-

ment network and data archive for aerosol characterization. Remote Sensing of Environment, 66(1): 1 – 16 [DOI: 10.1016/S0034 – 4257(98)00031 – 5]

Kaufman Y J, Boucher D, Tanré D, Chin M, Remer L A and Takemura T. 2005a. Aerosol anthropogenic component estimated from satellite data. Geophysical Research Letters, 32(17) [DOI: 10.1029/2005GL023125]

Kaufman Y J, Koren I, Remer L A, Tanré D, Ginoux P and Fan S. 2005b. Dust transport and deposition observed from the Terra-Moderate Resolution Imaging Spectroradiometer (MODIS) spacecraft over the Atlantic Ocean. Journal of Geophysical Research, 110(D10) [DOI: 10.1029/2003JD004436]

Li Z Q, Gu X, Wang L, Li D, Li K, Dubovik O, Schuster G, Goloub P, Zhang Y, Li L, Xie Y, Ma Y and Xu H. 2013. Aerosol physical and chemical properties retrieved from ground-based remote sensing measurements during heavy haze days in Beijing winter. Atmospheric Chemistry and Physics Discussions, 13(2): 5091 – 5122 [DOI: 10.5194/acpd – 13 – 5091 – 2013]

马锋敏, 高庆先, 周锁铨, 苏福庆, 康娜, 孙杰. 2008. **北京及周边地区一次典型大气污染过程的模拟分析**. **环境科学研究**, 21(1): 30 – 36

O'Neill N T, Eck T F, Smirnov A, Holben B N and Thulasiraman S. 2003. Spectral discrimination of coarse and fine mode optical depth. Journal of Geophysical Research, 108(D17) [doi]

任希岩, 吉东生, 王跃思, 胡波, 孙杨. 2008. **北京大气细粒子及其成分的浓度变化特征**. **地理信息科学**, 10(4): 426 – 430

Schuster G L, Lin B and Dubovik O. 2009. Remote sensing of aerosol water uptake. Geophysical Research Letters, 36(L03814) [DOI: 10.1029/2008GL036576]

孙家仁, 刘昱. 2008a. **中国区域气溶胶对东亚夏季风的可能影响(I): 硫酸盐气溶胶的影响**. **气候变化研究进展**, 4(2): 111 – 116

孙家仁, 刘昱. 2008b. **中国区域气溶胶对东亚夏季风的可能影响(II): 黑碳气溶胶及其与硫酸盐气溶胶的综合影响**. **气候变化研究进展**, 4(3): 161 – 166

Tanré D, Kaufman Y J, Holben B N, Chatenet B, Karnieli A, Lavenu F, Blarel L, Dubovik O, Remer L A and Smirnov A. 2001. Climatology of dust aerosol size distribution and optical properties derived from remotely sensed data in the solar spectrum. Journal of Geophysical Research, 106(D16): 18205 – 18217 [DOI: 10.1029/2000JD900663]

王玲, 李正强, 马荟, 李莉, 魏鹏, 田庆久. 2013. **基于太阳-太空辐射计的遥感观测反演北京冬季灰霾气溶胶化学成分含量**. **遥感学报**, 17(4): 944 – 958 [DOI: 10.11834/jrs.20133059]

Wang Y, Che H Z, Ma J Z, Wang Q, Shi G Y, Chen H B, Goloub P and Hao X J. 2009. Aerosol radiative forcing under clear, hazy, foggy, and dusty weather conditions over Beijing, China. Geophysical Research Letters, 36(6) [DOI: 10.1029/2009gl037181]

吴兑, 邓雪娇, 毕雪岩. 2007. **都市霾与雾的区分及粤港澳的灰霾天气观测预报预警标准**. **广东气象**, 29(2): 5 – 28

严鹏, 刘桂清, 周秀骥, 王京丽, 汤洁, 刘强, 王振发, 周怀刚. 2010. **上甸子秋冬季雾霾期间气溶胶光学特性**. **应用气象学报**, 21(3): 257 – 265

于兴娜, 李新妹, 登增然登, 德庆央宗, 袁帅. 2012. **北京雾霾天气期间气溶胶光学特性**. **环境科学**, 33(4): 1057 – 1062

张莹, 李正强. 2013. **利用细模态气溶胶光学深度估计** $PM_{2.5}$. **遥感学报**, 17(4): 929 – 943 [DOI: 10.11834/jrs.20133063]

中国气象局. 2010. **霾的观测和预报等级**. **北京: 中国气象出版社**